Structural metals at extremes

Amit Misra and Ludovic Thilly, Guest Editors

Designing structural materials for tailored response at extreme conditions is a grand challenge in materials research. Such materials can be made using either "top-down" or "bottom-up" processes to create nanostructured metals and composites that contain atomically designed interfaces that not only block dislocation slip but also attract, absorb, and annihilate point and line defects. Such multifunctional material systems are not just high in strength but also tolerant of damage at extremes of irradiation, temperature, and mechanical stresses, and hence have applications as structural materials in nuclear power and other energy, transportation and defense technologies. The exploration of these exceptional properties at extremes requires novel and unconventional methodologies, such as *in situ* experiments with high spatial and temporal resolution, complemented by simulation across multiple length and time scales.

Introduction

The topic of "materials under extreme environments" has received significant attention recently. Materials are key building blocks for the next generation of energy technologies, where they must feature enhanced performance at extremes of mechanical stress, strain, temperature, pressure, corrosive environments, particle radiation flux, and electric or magnetic fields.[1] For example, using supercritical steam significantly increases the efficiency of coal-fired power plants, but requires 50% higher operating temperatures and roughly double the operating pressure. Transportation applications, such as cars and aircraft, need lighter-weight and higher-strength structural materials to increase fuel efficiency and reduce CO_2 emission. For future nuclear-fission power plants, structural and cladding materials must perform at higher temperature and high dpa (displacements per atom). These increasingly extreme operating environments accelerate the aging process in materials, leading to reduced performance and eventually to failure.

Structural materials in defense, aerospace, construction, and other national-infrastructure applications also fail unpredictably, often at stresses less than 10% of the theoretical limit of strength for perfect crystals. Incremental changes in current structural materials may not produce the revolutionary breakthroughs needed for future applications. Innovative basic research that elucidates the fundamentals of how materials behave in extreme environments is required. Controlling the matter-extreme environment interactions can help researchers to develop revolutionary new materials that perform in predictable ways at stresses approaching the theoretical limit of material strength, on the order of 10% of the elastic modulus, extending lifetimes, increasing efficiencies, providing novel capabilities, and lowering costs.[1–3]

At a more fundamental level, the development of materials with a tailored response in extreme environments addresses one of the five grand challenges outlined in the recent Basic Energy Sciences Advisory Committee report[4] titled "Directing Matter and Energy: Five Challenges for Science and the Imagination": How do we design and perfect atom- and energy-efficient syntheses of revolutionary new forms of matter with tailored properties? Embodied in this grand challenge are specific science issues for structural materials at extremes, such as:

- How resistant to failure in extreme conditions of temperature, radiation, or environment exposure can we make a material?
- How do we make hard matter that heals damage or defects?
- How mechanically strong can we make materials yet keep them lightweight?

The field of "materials under extreme environments" is quite broad and may require more than one *MRS Bulletin* theme issue to capture the new developments. The focus of this issue is on metals, leaving out non-metals (ceramics for nuclear

Amit Misra, Los Alamos National Laboratory, New Mexico, USA; amisra@lanl.gov
Ludovic Thilly, Department of Physics and Mechanics of Materials, P-prime Institute, CNRS-University of Poitiers, SP2MI, Ave. Marie et Pierre Curie, 86962 Futuroscope, France; ludovic.thilly@univ-poitiers.fr

fuels, waste forms, and high-pressure synthesis of diamonds) and "chemistry at extremes" (e.g., chemistry of explosives at high-pressure, high strain rates). Keeping metals (especially nanostructured metals) as the focus, the set of articles in this issue highlights new developments in structural metals for radiation damage tolerance, shock, high magnetic fields, and high temperature stability. These articles capture three aspects of research in this field: (i) plastic deformation at extremes to synthesize bulk nano-metals and composites, (ii) performance of nano-metals and composites (regardless of synthesis method) in some form of extreme environment such as particle radiation, high temperatures, high strain rates, and high magnetic fields, and (iii) characterization methods (e.g., *in situ* x-ray diffraction or transmission electron microscopy [TEM]) for elucidation of damage processes under extreme environments.

Synthesis of new metal structures by severe plastic deformation bulk

During recent decades, the principal materials-design strategy has involved developing multifunctional structural materials with increased microstructure complexity. In this approach, the structural component also provides the functional property, such as reduced ~~of~~ mass, thermal insulation, electrical conduction, magnetic properties, acoustic damping, energy absorption, deformability, by adding selected new phases and refining the microstructure down to the nanometer scale. In this way, new nanocomposite materials have been developed, for instance, complex duplex steels or transformation-induced plasticity (TRIP) steels.[5] The mechanical properties of each phase of these complex materials are strongly influenced by the high surface-to-volume ratio of the nanograins. Their flow strength, which is dislocation-mediated at large grain size, is increased by the so-called "size effect" (smaller is stronger).[6–8] Moreover, the combination of different phases with different microstructure dimensions leads to complex co-deformation behavior.

Among the most promising fabrication techniques to obtain nanostructured metallic materials in the bulk form at the industrial scale are those based on severe plastic deformation (SPD), which by definition subjects materials to very large strains. In fact, researchers in this field talk in terms of "true strain," which is the natural logarithm of the ratio of initial and final dimensions. The true strain is equal to the traditional "engineering strain," or fractional change in dimension, only when these quantities are much less than one. In SPD, the true strain is typically larger than five, which breaks down the polycrystalline bulk material into crystalline units with dimensions of nanometers.

The article by Zhu et al. in this issue reviews the principal SPD techniques. Bulk nanostructured materials can be made using the severe deformations available in equal channel angular pressing (ECAP), high-pressure torsion (HPT), and accumulative roll bonding (ARB). Several variants of these SPD processes also exist: repetitive corrugation and straightening, co-shearing process, continuous confined strip shearing, twist extrusion, high-pressure tube twisting, asymmetric rolling, accumulative drawing, and bundling. Nanostructured surface layers can be created on bulk metals using the repetitive pummeling known as surface mechanical attrition treatment (SMAT).

This "top-down" approach of SPD is based on the accumulation of lattice defects (dislocations) to achieve microstructure refinement. It contrasts with a "bottom-up" approach, where nanostructured materials are synthesized atom-by-atom, layer-by-layer, or via consolidation of small clusters.[9] Metals are excellent candidates for SPD techniques, since they usually exhibit a ductile behavior at the strain rates and temperatures associated with these techniques. The details of the mechanisms involved in the grain refinement depend on the nature of the metals, such as crystallography, stacking fault energy, and strain hardening, and have been thoroughly studied during the past decades.[10,11]

The view emerging from the earlier research is that SPD involves different stages of glide and interaction of dislocations, leading to their accumulation with increasing strain (**Figure 1**a), until a heterogeneous microstructure is formed, composed of regions with high or low dislocation density (Figure 1b). Upon further straining of the structure, loose tangles transform into dislocation walls by annihilation of dislocations with opposite Burgers vectors (via combined glide, cross-slip, and climb processes), separating dislocation-free regions or subgrains (Figure 1c).

In SPD techniques, this process is pushed to the limits by reaching the extreme stages of work hardening,[10,11] where the thickness of the dislocation walls is further reduced (Figure 1d) until forming new grain boundaries. The formation of new grain boundaries suggests that grain refinement involves dynamic recovery of stored dislocations (Figure 1e). Along with the associated reduction of grain size, a typical feature of SPD-processed metals is the presence of a large fraction of grain boundaries (GBs) separating adjacent grains with crystallographic misorientation larger than 15°, referred to as high-angle grain boundaries (HAGBs).[11] HAGBs act as dislocation obstacles when the SPD-processed materials are subjected to service loading, giving them superior mechanical resistance.[12]

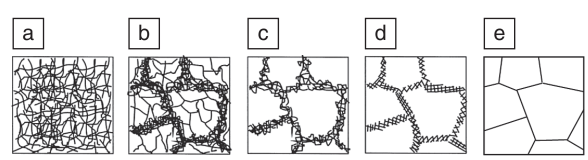

Figure 1. The main steps of grain refinement by severe plastic deformation (SPD). (a) Dislocations accumulate upon straining and (b) interact until forming a heterogeneous structure with high or low dislocation density regions. Further straining leads to the formation of (c) a typical microstructure with dislocation cells composed of dislocation walls separating dislocation-free regions (subgrains), the dislocation walls being (d) continuously refined until transformed into (e) grain boundaries when the SPD process is pushed to the limits to obtain a bulk ultrafine grain or nanostructured material.

The interest in studying SPD-processed materials is therefore twofold. First, the previously described microstructure refinement is a source for bulk materials with improved mechanical properties. Second, very large strains are imposed on the material in a confined geometry: the material is either forced to flow through a die with specific geometry (as in ECAP, ARB, and other variants) or to deform in a confined volume (as in HPT). In the case of SMAT, the material's surface is impacted by very energetic flying balls over a short period of time, and the bulk part of the material also confines the impacted region. In all cases, this confinement of metal flow leads to the creation of a complex stress state with intense hydrostatic and deviatoric components associated with high pressure and shear stresses. Such built-in pressure usually impedes massive fracture of the material, allowing copious plasticity.

Unique properties of nanostructured metals

Understanding how a metal responds to such severe and repeated deformation conditions is an important fundamental topic. Raabe et al. describe this issue in detail, with particular emphasis on the microstructure and the mechanical properties of metallic nanocomposites fabricated by SPD. By comparison to single-phase nanostructured metals, the study of composite materials is of interest since their mechanical properties generally result from a complex interplay between the properties of individual phases and the presence of interphase boundaries. In particular, internal stresses develop during co-deformation because of intra- and intergranular variations of plastic strain and have a strong impact on the strengthening mechanisms and macroscopic mechanical properties.

The first benefit in applying SPD to composite metals is the achievement of nanoscale phases leading to their improved mechanical strength. Among the oldest examples are the Damascene and Indian Wootz steels, or the steels obtained by pattern welding achieved by repeated folding in the early Middle Ages both in Europe and Asia.[13,14] Similar exceptional mechanical properties are found in modern materials such as steel cords and piano wires and are now recognized as the effect of microstructure refinement on the plasticity mechanisms.

Indeed, it is now established that microstructure refinement exerts a strong influence on the mechanical properties of materials, as a result of the coupling between two length scales. One scale is the characteristic length of the physical phenomenon involved (in the case of plasticity, the mean free path of dislocations and the average distance between dislocations). The other scale is the microstructural dimension (grain size, grain boundary width, obstacle spacing, and radius). The interaction of these two quantities leads to deviations from conventional behavior.[15,16]

The well-known Hall-Petch strengthening of polycrystalline materials is an example, in which a reduction of the grain size d (down to the micrometer regime) is accompanied by an increase of the yield stress, following a $d^{-1/2}$ dependence (**Figure 2**). With the development of new fabrication processes, the nanometer regime has been probed, and deviations from Hall-Petch strengthening have been recorded.

As GBs become more influential with grain-size reduction, the traditional plasticity mechanisms involving *intragrain* nucleation and propagation of dislocations become restricted. New strengthening mechanisms include deformation via uncorrelated dislocations (Orowan-type mechanism), with a grain-size dependence of the yield stress of $(1/d)\ln(d/b)$, where b is the length of the Burgers vector of the dislocations.[17–22] Another mechanism involves whisker-type behavior, with a $1/d$ dependence.[22,23] In the few-nanometer regime, a size-independent plateau in the yield stress is sometimes observed[21] and attributed to easy dislocation transmission across GBs, while in some nanocrystalline materials, a softening ("inverse" Hall-Petch effect[24]) has been reported as an indicator of diffusion processes or GB sliding associated with the large number of atoms located at GBs when the grain size is very small.

As pointed out in the article by Raabe et al., in nanocomposite metals, the heterophase interfaces provide an additional parameter to play with in the search for high-strength materials. Depending on the atomic species and the local crystallographic structure, these interfaces will transmit or trap dislocations, therefore modifying the strain-hardening behavior of the materials.

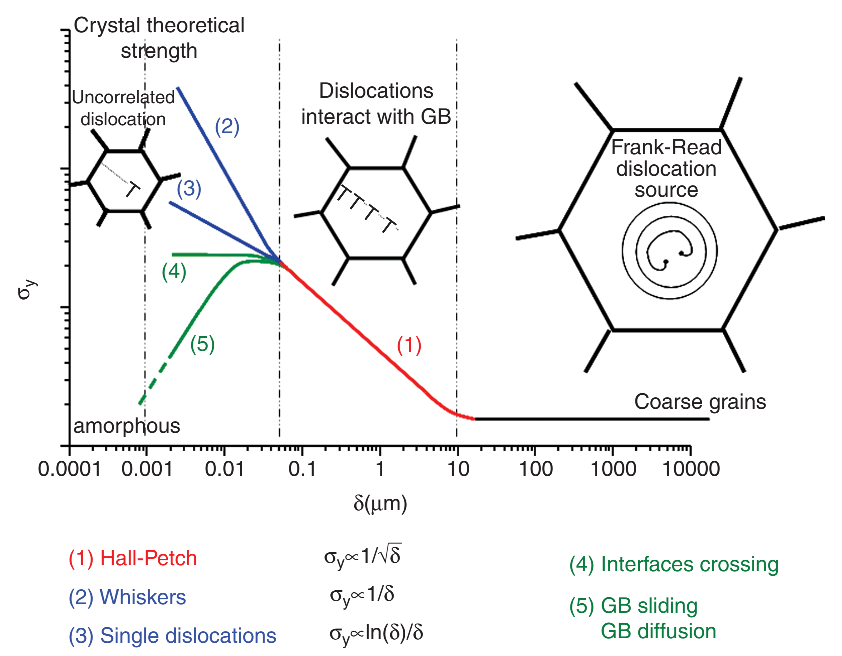

Figure 2. Schematic of the evolution of the yield strength σ_y in metals as a function of microstructure size δ (grain size in single phase materials or interface spacing in composites). The associated deformation mechanisms are described as well as the scaling laws that govern the elastic limit in the different regimes. GB, grain boundary.

It is clear that the concept of interface engineering will be a key issue in future development of nanocomposite materials, as discussed in the articles by Raabe et al. and Demkowicz et al.

Another remarkable feature exhibited by the nanostructured single phase or composite metals is the extension of the elastic-plastic transition, giving rise to a pronounced rounding of the stress-strain curves. This effect originates from very heterogeneous deformation taking place in these materials because of more-or-less extended grain- (or phase-) size distribution and complex internal stresses arising both from processing and from plastic incompatibilities between grains with different orientations relative to an externally applied stress.

At very small grain size, the probability that a grain experiences a plastic event (i.e., the emission of an individual dislocation at a GB, its gliding in the grain interior, and its absorption at the GB) is very small.[25,26] As a consequence, nanostructured materials exhibit an extended microplastic regime characterized by early strain hardening. Hence the conventional criterion used to define the onset of macroplasticity, a macroyield strain equal to 0.2%, appears meaningless since at such strain, only a very small portion of grains have deformed plastically.[25,26] This statement has been experimentally confirmed in nanocrystalline Ni, Cu/Ag multilayers, nanostructured Ni–Fe alloys, nanocomposite Cu/Nb wires, and nanocrystalline metal films. The amount of strain assigned to microplasticity was measured to significantly exceed the 0.2% convention for bulk metals.[27–32] This phenomenon must be taken into account to define a stress value that does not underestimate the onset of macroplasticity in nanostructured materials.

The second benefit of applying SPD to composite metals is to study their microstructure evolution when subjected to extreme strains, beyond most normal service conditions. After SPD, a large elastic energy is stored via internal stresses and lattice defects (dislocations, vacancies), a situation where the materials are far from thermodynamic equilibrium. In such conditions, unexpected phenomena are likely to appear at interfaces, such as mechanical alloying or amorphization, even in the case of highly immiscible phases. Raabe et al. review observations made possible by state-of-the-art characterization techniques at the atomic scale: high-resolution TEM and atom probe tomography are ideal experimental tools and are well complemented by simulation techniques.

The models proposed to explain these observations either invoke purely diffusion-driven mechanisms, defect-enhanced diffusion or interface roughening, and plasticity-driven mechanical mixing. Independent of the validity of the models, these observations lead to the following contradiction with what was described earlier. After SPD and (partial) dissolution of previously sharp interfaces, the nanocomposite metals continue to exhibit high strength. This phenomenon is still not fully understood, but it must be recognized in any process of interface engineering.

Nanostructured metals for high field magnets

As an illustration of how the SPD-processed nanocomposite metals are useful for applications that require extreme properties, we review the case of high–pulsed-field magnets. The generation of high magnetic fields (> 60 T) requires magnet winding materials with high electrical conductivity to minimize Ohmic heating effects. These fields are generally produced during a few milliseconds in pulsed magnets. At such fields, the Lorentz forces result in extreme Von Mises stresses on the winding material. At 60 T, the magnetic pressure is of the order of 1.5 GPa, and the Von Mises stress reaches 1 GPa; at 100 T, the magnetic pressure is 4 GPa, and the maximum stress on the magnet is larger than 2.2 GPa.[33–35] Multifunctional materials with high electrical conductivity and high strength are therefore needed to safely survive these harsh operating conditions in nondestructive magnets.

The high electrical conductivity requirement demands copper-based materials for the magnet application. Among these materials, only nanocomposite wires can combine low electrical resistivity with an elastic limit high enough to withstand the Von Mises stress previously described.[34] **Figure 3**

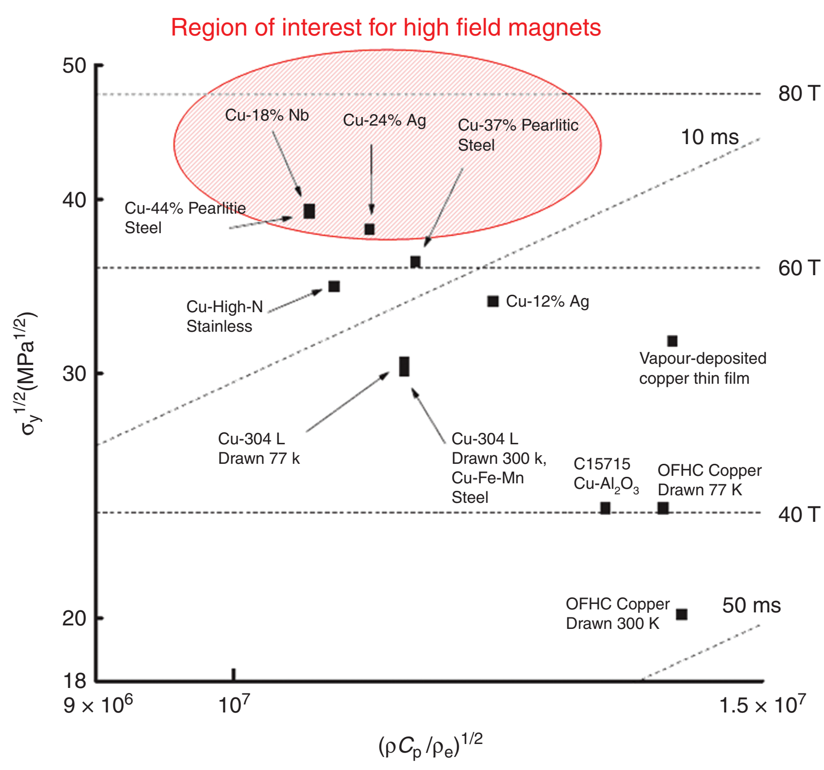

Figure 3. Materials-selection chart for high-field magnet development. Horizontal dashed lines indicate strength allowing a particular field intensity, while diagonal lines correspond to an allowable pulse duration. Only copper-based nanocomposite metals provide the necessary compromise between elastic limit ($\sigma_y^{1/2}$) and transport properties ($(\rho C_p/\rho_e)^{1/2}$), where ρ is the density, C_p is the volumetric heat capacity, and ρ_e is the electrical resistivity.[34]

is a materials-selection chart showing the relative position of different copper-based material classes (from bulk cold-drawn Cu to highly complex composites and alloys) with respect to the two limiting factors: strength, σ, plotted as $\sigma^{1/2}$, and a quantity that quantifies Ohmic heating. Heavily cold-drawn Cu/Nb (Cu-18%Nb) and Cu/Ag (Cu-24%Ag) wires are the best candidates for a 60T application; further improvements will still be required for higher fields.[34,36]

One of the candidates, labeled Cu-18%Nb in Figure 3, is continuous Cu/Nb nanocomposite wire, composed of an architectured multi-scale Cu matrix reinforced by Nb nanofilaments or nanotubes. The wires were fabricated by SPD with the accumulative drawing and bundling process (SPD methods are reviewed in the article by Zhu et al.). A series of hot-extrusion/cold drawing/bundling cycles are repeated n times ($n \leq 5$) to obtain conductors containing $N = 85^n$ Nb nanostructures with a known distribution, separated by channels of pure copper. The process induces a multiscale structure, as illustrated in **Figure 4** for a Cu/Nb wire.

This complex microstructure gives rise to extraordinary mechanical properties that have been studied by classical macroscopic tensile tests and nanoindentation, as well as *in situ* deformation in TEM and *in situ* deformation under neutron or synchrotron beam.[18,22,30] The ultimate tensile strength reaches 2 GPa at 77 K (i.e., five times that of cold-worked pure Cu) for nanocomposite wires with a diameter of 2.5 mm that contain Nb nanofilaments with a diameter of 142 nm.[18] The *in situ* experiments shed light on the specific elastic-plastic behavior of the different phases of the nanocomposites that are intimately connected to the local microstructure features (grain size). The micrometer-large Cu channels, with ultrafine grain structure (grain size from 200 nm to the micrometer range), exhibit strengthening following the Hall-Petch law; in the Cu nanochannels, the nucleation and propagation of dislocations are strongly affected by the reduced spacing between Cu-Nb interfaces, leading to a single-dislocation regime (Orowan-type) associated with increased yield stress; the Nb nanofilaments behave as whiskers with enhanced elastic limit.[22,30,37]

Although the required mechanical and electrical properties are achieved in wires fabricated at laboratory scale, their mass production and use in magnets is still limited by processing obstacles (one must ensure the production of several tens of meters of defect-free wires), difficulties in winding these wires into the needed coils (the gain in strength is usually associated with the loss of ductility, as for most SPD processed materials), and the poor knowledge of their fatigue properties when subjected to thermomechanical cycling in real magnets. As for most of the materials reviewed in the article by Raabe et al., there is clearly space for materials improvement. Innovative strategies, such as the design of architectured nanocomposite metals[3] or interface engineering, should bring interesting results in the near future.

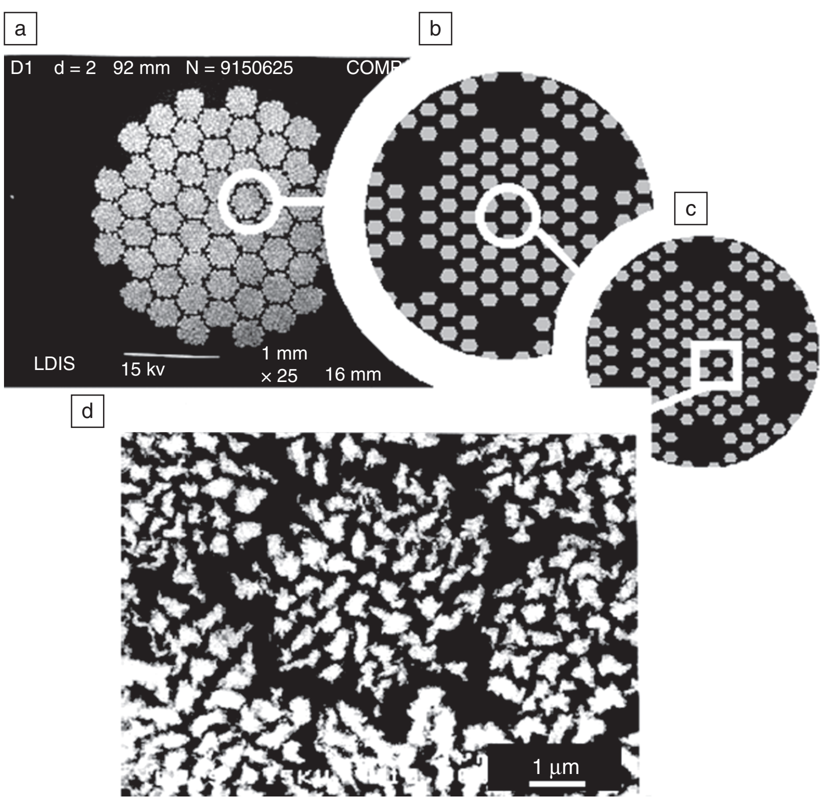

Figure 4. (a–c) Micrographs with successively higher magnification showing cross sections of the multiscale structure of Cu/Nb nanocomposite conductors for high-field pulsed magnets. (d) High magnification scanning electron micrograph showing Nb nanofilaments (white) embedded in the Cu matrix (black).[37]

Response of nano-metals and composites to extreme environments

The size effects on mechanical strength described previously for single-phase nanostructured metals also have been explored for thin films metallic multilayers[21,38–46] and nanotwinned fcc metals.[47–51] When the size refinement produces grain or interphase boundaries that are thermally stable[52] and can trap and annihilate point and line defects, the high strength can be combined with high damage tolerance in extreme environments. The article by Demkowicz et al. describes the atomic structures of boundaries that give rise to high damage tolerance.

Figure 5 and **6** show the increased damage tolerance of nanocomposites as compared with bulk metals. Bulk crystals or composites with ~~large~~ microstructure have very low strengths; nanostructuring leads to an increase in strength via the size effects discussed in Figure 2. For example, a Cu-Nb multilayer with an individual layer thickness of 5 nm has flow strength in excess of 2000 MPa, whereas the yield strengths of high purity, bulk single crystals of metals

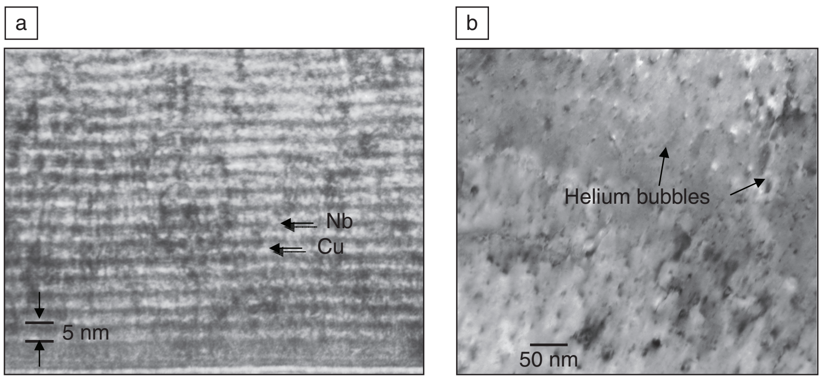

Figure 5. Transmission electron microscopy images of helium ion irradiated (a) 2.5 nm Cu–2.5 nm Nb nanolayered composite and (b) bulk Cu. Note the lack of dislocation loops, voids, and helium bubbles in the nanolayered composite while the bulk metal exhibits significant radiation damage.

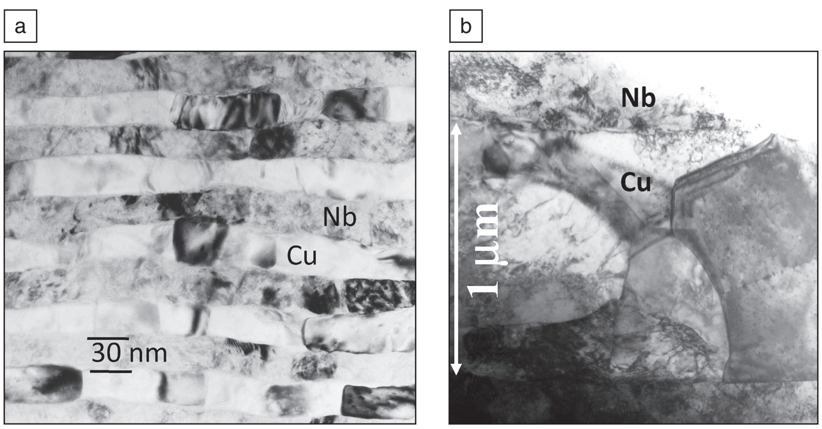

Figure 6. Transmission electron microscopy images of room-temperature rolled multilayers. (a) 75 nm Cu–75 nm Nb multilayer rolled to a layer thickness of 30 nm Cu–30 nm Nb and (b) 2 µm Cu–2 µm Nb multilayer rolled to a layer thickness of 1 µm Cu–1 µm Nb. Note the formation of dislocation cell structures in (b) and lack of dislocation cells, networks, and tangles in (a).

such as Cu are in the range of 10–50 MPa.[21,53] Bulk crystals also have very low damage tolerance. For example, particle irradiation leads to the formation of interstitials and vacancies. The highly mobile interstitials can escape to the surfaces or cluster with other interstitials and collapse into dislocation loops. The vacancies aggregate as well and trap transmutation products such as helium, resulting in cavities. Overall, these radiation-induced defect phenomena lead to an increase in the mechanical yield strength, embrittlement, and swelling.[54,55]

The article by Demkowicz et al. describes the atomic structures and energetics of interfaces that are super-sinks for radiation-induced defects, attracting, absorbing, and annihilating interstitials and vacancies, and thereby "self-healing" the material. As shown in Figure 5, for the same ion irradiation condition, pure Cu shows many defect agglomerates, but 2.5 nm Cu/2.5 nm Nb multilayers do not exhibit radiation damage.[56,57] These interfaces are stable under high-temperature ion irradiation as well.[58,59] Similar effects have been observed at special grain boundaries in single-phase metals.[60–65]

The same Cu-Nb interfaces are morphologically stable after room-temperature rolling to large plastic strains. Figure 6 shows that the micrometer-scale Cu-Nb multilayers developed dislocation-cell structures within the layers, leading to rotations away from the interface-plane normal. In contrast, the nanolayers (e.g., 75 nm layers rolled to 30 nm) showed no dislocation-cell structures and no rotation away from interface-plane normal.[66] Strain localization due to the formation of slip bands eventually leads to the initiation of cracks; hence, nanolayered materials with a more homogeneous distribution of slip and no accumulation of localized slip bands are more resistant to fracture.

Similarly, high strain-rate deformation increases the stress in a material to extremely high levels in a very short time. This results in excessive damage production, often via mechanisms such as twinning that are not activated at low stress levels.[67] The article by Rudd et al. in this issue discusses in more detail the behavior of materials at extremes of high strain rates. More work is needed to better understand the role of interfaces in controlling the behavior of materials at strain rate extremes.

All these findings suggest that nanostructured metals and composites can be designed to exhibit not just high strengths but also high damage tolerance, irrespective of whether the damage is introduced via plastic deformation or irradiation. The results reviewed here primarily highlight the fundamental mechanisms of defect interactions with interfaces in model systems. These concepts can underpin the design of advanced engineering materials such as nanocomposites of steel, such as those discussed in the article by Demkowicz et al. and in other recent reviews by Odette and co-workers.[68, 69] For materials issues with current engineering materials in nuclear power reactors, the reader is referred to an earlier *MRS Bulletin* issue edited by Was, Zinkle, and Guérin.[70]

Novel characterization methods for microstructure evolution at extremes

Although the microstructure of structural metals described in the different articles of this issue is well characterized in the as-processed state (from macroscopic to atomic scales), there is still a poorly known parameter: the microstructure stability of these materials in real service conditions. This stability is of crucial importance when the nanostructured materials are subjected to extreme conditions such as high strain rate deformation, fast heating, high-dose irradiation, and high-frequency thermal and/or mechanical cycling. In many cases, post-mortem analysis can be of great help for characterizing the final state of microstructure evolution, but the evolution path cannot always be elucidated. Simulation tools can fruitfully complement this approach;[71] however, the different simulation techniques have their own limitations, such as time and length scales of simulations, simplification of the microstructure, and validity of the interaction rules, and cannot fully replace experiments. Therefore to gain direct insight into the mechanisms governing the materials response under a given stimulus, *in situ* techniques have been widely developed during the last decades.[72,73]

The challenge for *in situ* characterization techniques is to obtain the best possible temporal and spatial resolutions simultaneously. The characterization of the temporal evolution is essential for the discrimination of the kinetics laws involved in the observed microstructure evolutions and to better define the material's lifetime: *in situ* time-resolved techniques necessitate a probe with sufficient flux to enable fast recording of high statistics data. The recording speed becomes a possible limitation when the observed processes are ultrafast. On the other hand, spatial resolution is necessary first to locate exactly where the modifications take place but also to characterize the involved mechanisms at the proper scale (atomic scale in most cases). *In situ* spatially resolved techniques necessitate a focused probe with very well-defined shape.

The article from Browning et al. in this issue reviews recent advances in the *in situ* characterization of microstructure evolution in metals under extreme conditions such as rapid thermal gradients, irradiation, shock-driven void formation, and extreme pressure using dynamic TEM (DTEM), *in situ* TEM ion irradiation, electron tomography, and synchrotron radiation (small-angle x-ray scattering). A detailed description of the modifications brought to the conventional instruments provides insight into the challenges that these experiments are facing. For example, in DTEM, the fast temporal resolution is achieved by using two different nanosecond lasers, one to start the transformation in the sample and one to create the imaging pulse of electrons by photoemission. For *in situ* irradiation, ion accelerators must be linked to TEM; for *in situ* shock loading, a synchrotron beamline (at the Advanced Photon Source, Argonne National Laboratory, USA) is equipped with a drive laser, specific x-ray detector while a special synchrotron fill pattern is used to obtain highest flux and shortest x-ray pulse.[74] Similarly, the Linac Coherent Light Source (LCLS) beam at SLAC National Accelerator Laboratory, with its high peak brightness, short pulse duration (<100 fs), and tunable wavelength in the x-ray energy range, provides revolutionary capabilities to study the transient behavior of matter in extreme conditions. The particular strength of the matter in extreme conditions (MEC) instrument is the combination of the unique LCLS beam with high-power optical laser beams to cover a broad range of extreme conditions such as intense pressure, temperature, stress, strain, and radiation.[75]

These developments in the *in situ* characterization techniques have been applied to a diverse range of problems, as described in the article by Browning et al. The crystallization of amorphous films (nucleation rate and growth speed), the radiation damage mechanisms, and the 3D defect density production in materials for nuclear-reactor applications (ferritic-martensitic and oxide-dispersion-strengthened steels) and the shock-generated submicron void formation in solids. These examples, and additional work reviewed in Reference 76, illustrate how the development of highly novel and unconventional methodologies pushes forward the frontiers of instrumentation and materials science.

Summary and future directions

Nanostructured metals and composites are known to be ultra-strong by virtue of the "smaller is stronger" trend. In addition to high strength, these materials can also be stable and damage tolerant at high irradiation doses at high temperatures, high strain rates, and large plastic strains. This unique combination of damage tolerance and high strength requires grain and/or interphase boundaries with atomic structures that make these boundaries strong obstacles to dislocations as well as strong sinks for point and line defects. Future developments of these multifunctional materials call for innovative strategies such as the design of architectured nanocomposite metals and interface engineering. These approaches necessitate detailed experimental and simulation inputs, in particular continuous development of highly novel and unconventional *in situ* experimental capabilities that push simultaneously the limits in spatial and temporal resolution. Such capabilities will help elucidate the damage production and recovery mechanisms at interfaces under extremes conditions of irradiation, stress, and temperature.

Acknowledgments

A.M. acknowledges support at LANL from the U.S. Department of Energy, Office of Science, Office of Basic Energy Sciences. L.T. acknowledges support from the French Research Agency under contract ANR-06-MAPR-0013.

References

1. U.S. Department of Energy, *Basic Research Needs for Materials under Extreme Environments* (BES Workshop on Basic Research Needs for Materials under Extreme Environments Report, 11–13 June 2007); www.sc.doe.gov/bes/reports/abstracts.html#MUEE.
2. J.D. Madden, *Science* **318**, 1094 (2007).
3. O. Bouaziz, Y. Bréchet, J.D. Embury, *Adv. Eng. Mater.* **1–2**, 10 (2008).
4. U.S. Department of Energy, *Directing Matter and Energy: Five Challenges for Science and the Imagination* (BESAC Grand Challenges report, 25 January 2005); www.sc.doe.gov/bes/reports/abstracts.html#GC.
5. O. Bouaziz, J.D. Embury, *Mater. Sci. Forum* **42**, 539 (2007).
6. K.S. Kumar, H. Van Swygenhoven, S. Suresh, *Acta Mater.* **51**, 5743 (2003).
7. J.R. Weertman, *MRS Bull.* **29**, 616 (2004).
8. H. Van Swygenhoven, J.R. Weertman, *Mater. Today* **9**, 24 (2006).
9. M.A. Meyers, A. Mishra, D.J. Benson, *Prog. Mater. Sci.* **51**, 427 (2006).
10. U.F. Kocks, H. Mecking, *Prog. Mater. Sci.* **48**, 171 (2003).
11. J.A. Wert, X. Huang, G. Winther, W. Pantleon, H.F. Poulsen, *Mater. Today* **10–9**, 24 (2007).
12. R.Z. Valiev, Y. Estrin, Z. Horita, T.G. Langdon, M.J. Zehetbauer, Y.T. Zhu, *JOM* **58**, 33 (2006).

13. J.D. Verhoeven, *Metallography* **20**, 145 (1987).
14. W. Kochmann, M. Reibold, R. Goldberg, W. Hauffe, A.A. Levin, D.C. Meyer, T. Stephan, H. Müller, A. Belger, P. Paufler, *J. Alloys Comp.* **372**, L15 (2004).
15. E. Arzt, *Acta Mater.* **46**, 5611 (1998).
16. H. Gleiter, *Acta Mater.* **48**, 1 (2000).
17. K.S. Kumar, H. Van Swygenhoven, S. Suresh, *Acta Mater.* **51**, 5743 (2003).
18. L. Thilly, F. Lecouturier, J. Von Stebut, *Acta Mater.* **50**, 5049 (2002).
19. J. Gil Sevillano, *J. Phys. III* **1**, 967 (1991).
20. J.D. Embury, J.P. Hirth, *Acta Mater.* **42** (6), 2051 (1994).
21. A. Misra, J.P. Hirth, R.G. Hoagland, *Acta Mater.* **53**, 4817 (2005).
22. L. Thilly, O. Ludwig, M. Véron, F. Lecouturier, J.P. Peyrade, S. Askénazy, *Philos. Mag. A* **82** (5), 925 (2002).
23. S.S. Brenner, *J. Appl. Phys.* **27** (12), 1484 (1956).
24. A.H. Chokshi, A. Rosen, J. Karch, H. Gleiter, *Scripta Mater.* **23**, 1679 (1989).
25. G. Saada, *Mater. Sci. Eng. A* **400–401**, 146 (2005).
26. G. Saada, *Philos. Mag.* **85**, 3003 (2005).
27. S. Brandstetter, H. Van Swygenhoven, S. Van Petegem, B. Schmitt, R. Maaß, P.M. Derlet, *Advanced Mater.* **18**, 1545 (2006).
28. G. Saada, M. Verdier, G.F. Dirras, *Philos. Mag.* **87**, 4875 (2007).
29. H. Li, H. Choo, Y. Ren, T.A. Saleh, U. Lienert, P.K. Liaw, F. Ebrahimi, *Phys. Rev. Lett.* **101**, 015502 (2008).
30. L. Thilly, S. Van Petegem, P.O. Renault, F. Lecouturier, V. Vidal, B. Schmitt, H. Van Swygenhoven, *Acta Mater.* **57**, 3157 (2009).
31. J. Rajagopalan, C. Rentenberger, H.P. Karnthale, G. Dehm, M.T.A. Saif, *Acta Mater.* **58**, 4772 (2010).
32. C.C. Aydiner, D.W. Brown, N.A. Mara, J. Almer, A. Misra, *Appl. Phys. Lett.* **94**, 031906 (2009).
33. S. Askénazy, *Phys. B* **211**, 56 (1995).
34. K. Spencer, F. Lecouturier, L. Thilly, J.D. Embury, *Adv. Eng. Mater.* **6**, 290 (2004).
35. L. Thilly, F. Lecouturier, *Nanomaterials and Nanochemistry: High Field Coils*, (Springer, New York, 2007), p. 685.
36. J. Freudenberger, J. Lyubimova, A. Gaganov, H. Witte, A.L. Hickman, H. Jones, M. Nganb, *Mater. Sci. Eng. A* **527**, 2004 (2010).
37. L. Thilly, V. Vidal, S. Van Petegem, U. Stuhr, F. Lecouturier, P.O. Renault, H. Van Swygenhoven, *Appl. Phys. Lett.* **88**, 191906 (2006).
38. W.D. Nix, *Math. Mech. Solids* **14**, 207 (2009).
39. S.M. Han, M.A. Phillips, W.D. Nix, *Acta Mater.* **57**, 4473 (2009).
40. J. Wang, R.G. Hoagland, A. Misra, *Scripta Mater.* **60**, 1067 (2009).
41. I.N. Mastorakos, H.M. Zbib, D.F. Bahr, *Appl. Phys. Lett.* **94**, 173114 (2009).
42. P.M. Anderson, J.S. Carpenter, *Scripta Mater.* **62**, 325 (2010).
43. Y.P. Li, G.P. Zhang, *Acta Mater.* **58**, 3877 (2010).
44. A.C. Lewis, C. Eberl, K.J. Hemker, T.P. Weihs, *J. Mater. Res.* **23**, 376 (2008).
45. B.M. Clemens, H. Kung, S.A. Barnett, *MRS Bull.* **24**, 20 (1999).
46. R.C. Cammarata, *Scripta Mater.* **50**, 751 (2004).
47. L. Lu, X. Chen, X. Huang, K. Lu, *Science* **323**, 607 (2009).
48. T. Zhu, J. Li, A. Samanta, H.G. Kim, S. Suresh, *Proc. Nat. Acad. Sci. U.S.A.* **104**, 3031 (2007).
49. O. Anderoglu, A. Misra, J. Wang, R.G. Hoagland, J.P. Hirth, X. Zhang, *Int. J. Plast.* **26**, 875 (2010).
50. F. Sansoz, H. Huang, D.H. Warner, *JOM* **60**, 79 (2008).
51. C.J. Shute, B.D. Myers, S. Xie, T.W. Barbee Jr, A.M. Hodge, J.R. Weertman, *Scripta Mater.* **60**, 1073 (2009).
52. A. Misra, R.G. Hoagland, H. Kung, *Philos. Mag.* **84**, 1021 (2004).
53. N.A. Mara, D. Bhattacharyya, P. Dickerson, R.G. Hoagland, A. Misra, *Appl. Phys. Lett.,* **92**, 231901 (2008).
54. D.L. Porter, F.A. Garner, *J. Nucl. Mater.* **159**, 114 (1988).
55. R.J. Kurtz, F. Gao, H.L. Heinisch, B.D. Wirth, G.R. Odette, T. Yamamoto, *JOM* **56**, 263 (2004).
56. A. Misra, M.J. Demkowicz, X. Zhang, R.G. Hoagland, *JOM* **59**, 62 (2007).
57. X. Zhang, N. Li, O. Anderoglu, H. Wang, J.G. Swadener, T. Hochbauer, A. Misra, R.G. Hoagland, *Nucl. Instrum. Methods Phys. Res., Sect. B* **261** (1–2), 1129 (2007).
58. T. Hochbauer, A. Misra, K. Hattar, R.G. Hoagland, *J. Appl. Phys.* **98**, 123516 (2005).
59. K. Hattar, M.J. Demkowicz, A. Misra, I.M. Robertson, R.G. Hoagland, *Scripta Mater.* **58**, 541 (2008).
60. B.N. Singh, *Philos. Mag.* **28**, 1409 (1973).
61. N. Nita, R. Schaeublin, M. Victoria, R.Z. Valiev, *Philos. Mag.* **85**, 723 (2005).
62. M. Rose, A.G. Balogh, H. Hahn, *Nucl. Instrum. Methods Phys. Res., Sect. B* **127/128**, 119 (1997).
63. M. Samaras, P.M. Derlet, H. van Swygenhoven, M. Victoria, *Phys. Rev. Lett.* **88**, 125505 (2002).
64. H.L. Hienisch, F. Gao, R.J. Kurtz, *J. Nucl. Mater.* **329–333**, 924 (2004).
65. X.M. Bai, A.F. Voter, R.G. Hoagland, M. Nastasi, B.P. Uberuaga, *Science* **327**, 1631 (2010).
66. A. Misra, J.P. Hirth, R.G. Hoagland, J.D. Embury, H. Kung, *Acta Mater.* **52**, 2387 (2004).
67. F. Cao, I.J. Beyerlein, F.L. Addessio, B.H. Sencer, C.P. Trujillo, E.K. Cerreta, G.T. Gray III, *Acta Mater.* **58**, 549 (2010).
68. G.R. Odette and D.T. Hoelzer, *JOM*, September, 84 (2010).
69. G.R. Odette, M.J. Alinger, B.D. Wirth, *Annual Review of Materials Research*, **38**, 471 (2008).
70. G.S. Was, S.J. Zinkle, Y. Guérin, *MRS Bull.* **34** (1), 10 (2009).
71. H. Huang, H. Van Swygenhoven, *MRS Bull.* **34** (3), 160 (2009).
72. I.M. Robertson, P.J. Ferreira, G. Dehm, R. Hull, E.A. Stach, *MRS Bull.* **33** (2), 122 (2008).
73. M. Legros, D.S. Gianola, C. Motz, *MRS Bull.* **35** (5), 354 (2010).
74. D.H. Kalantar, G.W. Collins, J.D. Colvin, J.H. Eggert, J. Hawreliak, H.E. Lorenzana, M.A. Meyers, R.W. Minich, K. Rosolankova, M.S. Schneider, J.S. Stölken, J.S. Wark, *Int. J. Impact Eng.* **33**, 343 (2006).
75. SLAC National Accelerator Laboratory, https://slacportal.slac.stanford.edu/sites/lcls_public/instruments/mec/Pages/default.aspx.
76. P.G. Evans, S.J.L. Billinge, *MRS Bull.* **35** (6), 495 (2010). □